

University of California - Davis

UCD-96-16

May 1996

**Physics Motivations for a Muon Collider \***

John F. Gunion

*Davis Institute for High Energy Physics**University of California at Davis, Davis, CA 95616, USA***Abstract**

Future muon colliders will have remarkable capability for revealing and studying physics beyond the Standard Model. A first muon collider with variable c.m. energy in the range  $\sqrt{s} = 100$  to 500 GeV provides unique opportunities for discovery and factory-like production of Higgs bosons in the  $s$ -channel. For excellent (but achievable) machine energy resolution, the total width and  $\mu^+\mu^-$  coupling of a SM-like Higgs boson with mass  $\lesssim 2m_W$  (as particularly relevant to supersymmetric/GUT models) can be directly measured with substantial precision. Multiplication of measured branching ratios by the total width yields the corresponding couplings. As a result, the light CP-even SM-like Higgs of the minimal supersymmetric model can be distinguished from the Higgs of the minimal Standard Model over a larger portion of supersymmetric parameter space than otherwise possible. Scan discovery and detailed measurements of total widths and some partial widths of the heavier CP-even and CP-odd Higgs bosons of the minimal supersymmetric model are possible for Higgs masses up to the maximum  $\sqrt{s}$ . The excellent energy resolution, absence of beamstrahlung and mild bremsstrahlung at the first muon collider would allow increased precision for the measurement of  $m_t$  and  $m_W$  via  $t\bar{t}$  and  $W^+W^-$  threshold studies. A multi-TeV  $\mu^+\mu^-$  collider would open up the realm of physics above the 1 TeV scale. Pair production of supersymmetric particles up to masses even higher than consistent with naturalness would be possible, guaranteeing that the heavier gauginos and possibly very massive squarks would be abundantly produced and that their properties could be studied. Very importantly, the multi-TeV collider would guarantee our ability to perform a detailed study of a strongly-interacting scenario of electroweak symmetry breaking, including a bin-by-bin measurement of the vector boson pair mass spectrum in all relevant weak isospin channels.

---

\*To appear in *Proceedings of the Rencontres de Physique de la Vallée d'Aoste, 1996*. Based on work performed in collaboration with V. Barger, M. Berger, and T. Han.

# 1 Introduction

There is increasing interest in the possible construction of a  $\mu^+\mu^-$  collider [1,2,3,4]. The expectation is that a muon collider with energy and integrated luminosity comparable to or superior to those attainable at  $e^+e^-$  colliders can be achieved [6,7,8]. Two possible  $\mu^+\mu^-$  machines have been discussed as design targets and are being actively studied [2,3,4]:

- (i) A first muon collider (FMC) with low c. m. energy ( $\sqrt{s}$ ) between 100 and 500 GeV and  $\mathcal{L} \sim 2-5 \times 10^{33} \text{ cm}^{-2} \text{ s}^{-1}$  delivering an annual integrated integrated luminosity  $L \sim 20 - 50 \text{ fb}^{-1}$ .
- (ii) A next muon collider (NMC) with high  $\sqrt{s} \gtrsim 4 \text{ TeV}$  and  $\mathcal{L} \sim 10^{35} \text{ cm}^{-2} \text{ s}^{-1}$  giving  $L \sim 1000 \text{ fb}^{-1}$  yearly.

Schematic designs for a muon collider and other machine and detector details can be found in the talk by A. Tollestrup in these same proceedings. Several surveys [9,11] discuss the remarkable potential of muon colliders for revealing and studying new types of physics beyond the Standard Model. Here, I present an overview of the available results.

The physics possibilities at a  $\mu^+\mu^-$  collider include those of an  $e^+e^-$  collider with the same energy and luminosity. However, the muon collider program would supplement and be highly complementary to that at an electron collider in two ways.

- The physics program at the lower energy muon collider could be focused on the studies that cannot be performed at an existing electron collider of similar energy and luminosity. Indeed, the muon collider's unique abilities in Higgs physics and precision threshold analyses can only be fully exploited by devoting all the luminosity to these very specific goals.
- New phenomena observed at the multi-TeV muon collider might be much more easily unravelled if data from an electron collider at lower energy is available. For example, a complex supersymmetric particle spectrum will be most easily sorted out by having substantial luminosity at both a lower energy electron collider and the high energy muon collider.

Thus, it will be very advantageous if the technologically more advanced planning for an electron collider results in its early construction. Similarly, the muon collider program will benefit enormously from existing LHC data. Thus, my focus will be on what can be done at a muon collider that goes beyond and benefits from possibly existing electron collider and LHC results.

The advantages of a muon collider can be summarized briefly as follows:

- The muon is significantly heavier than the electron, and therefore couplings to Higgs bosons are enhanced making possible their discovery and study in the  $s$ -channel production process.

- Extending the energy reach of a muon collider well beyond the 1 TeV range is possible. Large luminosity is achieved for moderate beam size by storing multiple bunches in the final storage ring and having a large number of turns of storage per cycle. Radiative losses in the storage ring are small due to the large muon mass.
- The muon collider can be designed to have much finer energy resolution than an  $e^+e^-$  machine. The energy profile of the beam is expected to be roughly Gaussian in shape, and the rms deviation  $R$  is expected to naturally lie in the range  $R = 0.04\%$  to  $0.08\%$  [10]. Additional cooling could further sharpen the beam energy resolution to  $R = 0.01\%$ . The monochromaticity of the beams is critically important for some of the physics that can be done at a  $\mu^+\mu^-$  collider.
- At a muon collider,  $\mu^+\mu^+$  and  $\mu^-\mu^-$  collisions are likely to be as easily achieved as  $\mu^+\mu^-$  collisions.

Further complementarity between the muon and electron colliders results from two slight drawbacks of a muon collider. The first is that substantial polarization of the beams can probably not be achieved without sacrificing luminosity. The second drawback is that the  $\gamma\gamma$  and  $\mu\gamma$  collider options are probably not feasible (see [11]), whereas the corresponding options would be feasible at future linear electron colliders.

## 2 $s$ -channel Higgs Physics

If Higgs bosons exist, a complete study of all their properties will be a crucial goal of the next generation of colliders. A muon collider could be an especially valuable and, perhaps, crucial tool.

The simplest Higgs sector is that of the Standard Model (SM) with one Higgs boson ( $h_{SM}$ ). However, the naturalness and hierarchy problems that arise in the SM and the failure of grand unification of couplings in the SM suggest that the Higgs sector will be more complex. Supersymmetry is an especially attractive candidate theory in that it solves the naturalness and hierarchy problems (for a sufficiently low scale of supersymmetry breaking) and in that scalar bosons, including Higgs bosons, are on the same footing as fermions as part of the particle spectrum. The minimal supersymmetric model (MSSM) is the simplest SUSY extension of the SM. In the MSSM, every SM particle has a superpartner. In addition, the minimal model contains exactly two Higgs doublets. At least two Higgs doublet fields are required in order that both up and down type quarks be given masses without breaking supersymmetry (and also to avoid anomalies in the theory). Exactly two doublets allows unification of the SU(3), SU(2) and U(1) coupling constants. (Extra Higgs singlet fields are allowed by unification, but are presumed absent in the MSSM.) For two Higgs doublets and no Higgs singlets, the Higgs spectrum comprises 5 physical Higgs bosons

$$h^0, H^0, A^0, H^+, H^- . \quad (1)$$

The quartic couplings in the MSSM Higgs potential are related to the electroweak gauge couplings  $g$  and  $g'$  and the tree-level Higgs mass formulas imply an upper bound on the mass of the lightest Higgs boson,  $m_{h^0} \leq m_Z$ . At one loop, the radiative correction to the mass of the lightest Higgs state depends on the top and stop masses

$$\delta m_{h^0}^2 \simeq \frac{3g^2}{8\pi^2 m_W^2} m_t^4 \ln \left( \frac{m_{\tilde{t}_1} m_{\tilde{t}_2}}{m_t^2} \right). \quad (2)$$

Two-loop corrections are also significant. The resulting ironclad upper bounds on the possible mass of the lightest Higgs boson are

$$\begin{aligned} m_{h^0} &\lesssim 130 \text{ GeV MSSM,} \quad m_{h^0} \lesssim 150 \text{ GeV any SUSY GUT,} \\ m_{h^0} &\lesssim 200 \text{ GeV any model with GUT and desert.} \end{aligned}$$

In the largest part of parameter space, e.g.  $m_{A^0} > 150 \text{ GeV}$  in the MSSM, the lightest Higgs boson has fairly SM-like couplings. The critical conclusion from the muon collider point of view is that SUSY/GUT models predict that the SM-like Higgs boson required to guarantee gauge boson scattering unitarity is very likely to have mass  $\lesssim 2m_W$ . A muon collider has unique capabilities for studying a SM-like Higgs boson that is too light to actually decay to gauge boson pairs. In contrast, a SM-like Higgs boson with mass such that  $WW$  decays are allowed is not easily observed at a muon collider.

The first discovery of a light Higgs boson is likely to occur at the LHC which might be operating for several years before a next-generation lepton collider is built. Following its discovery, interest will focus on measurements of its mass, total width, and partial widths. A first question then is what could be accomplished at the Large Hadron Collider (LHC) or the Next Linear Collider (NLC) in this regard. The LHC collaborations report that the Higgs boson is detectable in the mass range  $50 \lesssim m_h \lesssim 150 \text{ GeV}$  via its  $\gamma\gamma$  decay mode. The mass resolution is expected to be  $\lesssim 1\%$ . At the NLC the Higgs boson is produced in the Bjorken process  $e^+e^- \rightarrow Z^* \rightarrow Zh$  and the  $h$  can be studied through its dominant  $b\bar{b}$  decay. At the NLC, the mass resolution is strongly dependent on the detector performance and signal statistics. Studies for an SLD-type detector [12] and the “super”-LC detector [13,14] have been performed. For a Higgs boson with Standard Model couplings and mass  $\lesssim 2m_W$  this gives a Higgs mass determination of

$$\Delta m_{h_{SM}} \simeq 400 \text{ MeV} \left( \frac{10 \text{ fb}^{-1}}{L} \right)^{1/2}, \quad (3)$$

for the SLD-type detector. Thus, from both LHC and NLC data we will have a very good determination of the mass of a SM-like Higgs boson. This will be important for maximizing the ability of a muon collider to perform precision measurements of the Higgs total width and partial widths, as necessary to distinguish between the predictions of the SM Higgs boson  $h_{SM}$  and the MSSM Higgs boson  $h^0$ . Can the total and partial widths be measured at other machines? This is a complicated

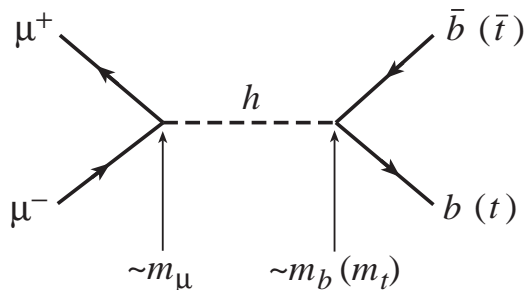


Figure 1: Feynman diagram for  $s$ -channel production of a Higgs boson.

question since each machine contributes different pieces to the puzzle. The bottom line [15] is that the LHC, NLC, and  $\gamma\gamma$  colliders each measure interesting couplings and/or branching ratios, but their ability to detect deviations due to the differences between the  $h^0$  and  $h_{SM}$  is limited to  $m_{A^0} \lesssim 300$  GeV. Further, a model-independent study of all couplings and widths requires all three machines with consequent error propagation problems.

The  $s$ -channel process  $\mu^+\mu^- \rightarrow h \rightarrow b\bar{b}$  shown in Fig. 1 is uniquely suited to several definitive precision Higgs boson measurements [16,17]. Detecting and studying the Higgs boson in the  $s$ -channel would require that the machine energy be adjusted to correspond to the Higgs mass. Since the storage ring is only a modest fraction of the overall muon collider cost [18], a special-purpose ring could be built to optimize the luminosity near the Higgs peak.

The  $s$ -channel Higgs phenomenology is set by the  $\sqrt{s}$  rms Gaussian spread denoted by  $\sigma_{\sqrt{s}}$ . A convenient formula for  $\sigma_{\sqrt{s}}$  is

$$\sigma_{\sqrt{s}} = (7 \text{ MeV}) \left( \frac{R}{0.01\%} \right) \left( \frac{\sqrt{s}}{100 \text{ GeV}} \right). \quad (4)$$

A crucial consideration is how this natural spread in the muon collider beam energy compares to the width of the Higgs bosons, given in Fig. 2. In particular, a direct scan measurement of the Higgs width requires a beam spread comparable to the width. The narrowest Higgs boson widths are those of a light SM Higgs boson with mass  $\lesssim 100$  GeV. In the limit where the heavier MSSM Higgs bosons become very massive, the lightest supersymmetric Higgs typically has a mass of order 100 GeV and has couplings that are sufficiently SM-like that its width approaches that of a light  $h_{SM}$  of the same mass. In either case, the discriminating power of a muon collider with a very sharp energy resolution would be essential for a direct width measurement. A direct measurement of the width is not possible at any other machine.

To quantify just how good the resolution must be, consider Fig. 2 which shows that for typical muon beam resolution ( $R = 0.06\%$ )

$$\sigma_{\sqrt{s}} \gg \Gamma_{h_{SM}}, \text{ for } m_{h_{SM}} \sim 100 \text{ GeV}, \quad (5)$$

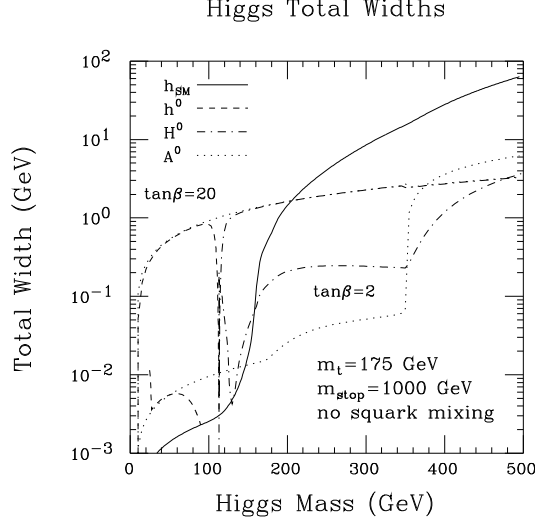


Figure 2: Total width versus mass of the SM and MSSM Higgs bosons for  $m_t = 175$  GeV. In the case of the MSSM, we have plotted results for  $\tan\beta = 2$  and 20, taking  $m_{\tilde{t}} = 1$  TeV and including two-loop corrections following Refs. [19,20] neglecting squark mixing; SUSY decay channels are assumed to be absent.

$$\sigma_{\sqrt{s}} \sim \Gamma_{h^0}, \text{ for } m_{h^0} \text{ not near } m_{h^0}^{\max}, \quad (6)$$

$$\sigma_{\sqrt{s}} \lesssim \Gamma_{H^0}, \Gamma_{A^0}, \text{ at moderate } \tan\beta, \quad (7)$$

for  $m_{H^0, A^0} \sim 400$  GeV ,

$$\ll \Gamma_{H^0}, \Gamma_{A^0}, \text{ at large } \tan\beta, \quad (8)$$

for  $m_{H^0, A^0} \sim 400$  GeV .

To be sensitive to  $\Gamma_{h_{SM}}$ , a resolution  $R \sim 0.01\%$  is mandatory. This is an important conclusion given that such a small resolution requires early consideration in the machine design.

The  $s$ -channel Higgs resonance cross section is

$$\sigma_h = \frac{4\pi\Gamma(h \rightarrow \mu\mu)\Gamma(h \rightarrow X)}{(\hat{s} - m_h^2)^2 + m_h^2[\Gamma_h^{\text{tot}}]^2}, \quad (9)$$

where  $\hat{s} = (p_{\mu^+} + p_{\mu^-})^2$  is the c. m. energy squared of the event,  $X$  denotes a final state and  $\Gamma_h^{\text{tot}}$  is the total width. The effective cross section is obtained by convoluting this resonance form with the Gaussian distribution of width  $\sigma_{\sqrt{s}}$  centered at  $\sqrt{s}$ . When the Higgs width is much smaller than  $\sigma_{\sqrt{s}}$ , the effective signal cross section result for  $\sqrt{s} = m_h$ , denoted by  $\bar{\sigma}_h$ , is

$$\bar{\sigma}_h = \frac{2\pi^2\Gamma(h \rightarrow \mu\mu)BF(h \rightarrow X)}{m_h^2} \times \frac{1}{\sigma_{\sqrt{s}}\sqrt{2\pi}}. \quad (10)$$

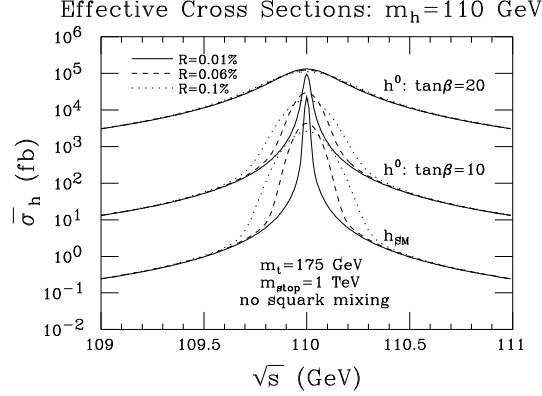


Figure 3: The effective cross section,  $\bar{\sigma}_h$ , obtained after convoluting  $\sigma_h$  with the Gaussian distributions for  $R = 0.01\%$ ,  $R = 0.06\%$ , and  $R = 0.1\%$ , is plotted as a function of  $\sqrt{s}$  taking  $m_h = 110$  GeV.

In the other extreme, where the Higgs width is much broader than  $\sigma_{\sqrt{s}}$ , at  $\sqrt{s} = m_h$  we obtain

$$\bar{\sigma}_h = \frac{4\pi BF(h \rightarrow \mu\mu)BF(h \rightarrow X)}{m_h^2}. \quad (11)$$

We note from Eq. (11) that if  $\Gamma_h^{\text{tot}}$  is large and  $BF(h \rightarrow \mu\mu)$  small, as for a SM Higgs with large  $WW$  decay width, then  $\bar{\sigma}_h$  is greatly suppressed and observation of the  $h$  would be difficult at the muon collider. Figure 3 illustrates the result of the convolution as a function of  $\sqrt{s}$  for  $\sqrt{s}$  near  $m_h$  in the three situations:  $\Gamma_h^{\text{tot}} \ll \sigma_{\sqrt{s}}$ ,  $\Gamma_h^{\text{tot}} \sim \sigma_{\sqrt{s}}$  and  $\Gamma_h^{\text{tot}} \gg \sigma_{\sqrt{s}}$ . We observe that small  $R$  greatly enhances the peak cross section for  $\sqrt{s} = m_h$  when  $\Gamma_h^{\text{tot}} \ll \sigma_{\sqrt{s}}$ , as well as providing an opportunity to directly measure  $\Gamma_h^{\text{tot}}$ .

As an illustration, suppose  $m_h \sim 110$  GeV and  $h$  is detected in  $e^+e^- \rightarrow Zh$  or  $\mu^+\mu^- \rightarrow Zh$  with mass uncertainty  $\delta m_h \sim \pm 0.8$  GeV (obtained with luminosity  $L \sim 1 \text{ fb}^{-1}$ ). For a standard model Higgs of this mass, the width is about 3.1 MeV. How many scan points and how much luminosity are required to zero in on  $m_{h_{SM}}$  to within one rms spread  $\sigma_{\sqrt{s}}$ ? For  $R = 0.01\%$  ( $R = 0.06\%$ ),  $\sigma_{\sqrt{s}} \sim 7.7$  MeV ( $\sim 45$  MeV) and the number of scan points required to cover the 1.6 GeV mass zone at intervals of  $\sigma_{\sqrt{s}}$  will be 230 (34), respectively. The luminosity required to observe (or exclude) the Higgs at each point is  $L \gtrsim 0.01 \text{ fb}^{-1}$  ( $L \gtrsim 0.3 \text{ fb}^{-1}$ ) for  $R = 0.01\%$  ( $R = 0.06\%$ ). Thus, the total luminosity required to zero in on the Higgs will be  $\sim 2.3 \text{ fb}^{-1}$  ( $\sim 10.2 \text{ fb}^{-1}$ ) in the two cases. Thus, the  $\mu^+\mu^-$  collider should be constructed with the smallest possible  $R$  value with the proviso that the number of  $\sqrt{s}$  settings can be correspondingly increased for the required scan. It must be possible to quickly and precisely adjust the energy of the  $\mu^+\mu^-$  collider to do the scan.

To measure the width of a SM-like Higgs boson, one would first determine  $m_h$

to within  $d\sigma_{\sqrt{s}}$  with  $d \lesssim 0.3$  and then measure the cross section accurately at the wings (roughly  $\pm 2\sigma_{\sqrt{s}}$  away from the central measurement) of the excitation peak, see Fig. 3. The two independent measurements of  $\sigma_{\text{wings}}/\sigma_{\text{peak}}$  give improved precision for the Higgs mass and determine the Higgs width in a model-independent manner [since the partial decay rates in the numerator in Eq. (9) cancel out]. It is advantageous to put about 2 1/2 times as much luminosity on each of the wings as at the peak. The detailed procedure is given in [17]. Accurate determination of the background from measurements farther from the resonance or from theoretical predictions is required. For  $R = 0.01\%$ , a total luminosity for the peak and wing measurements of  $2 \text{ fb}^{-1}$  ( $200 \text{ fb}^{-1}$ ) would be required to measure  $\Gamma_h^{\text{tot}}$  with an accuracy of  $\pm 30\%$  for  $m_h = 110 \text{ GeV}$  ( $m_h = m_Z$ ). An accuracy of  $\pm 10\%$  for  $\Gamma_h^{\text{tot}}$  could be achieved for reasonable luminosities provided  $m_h$  is not near  $m_Z$ .

It must be stressed that the ability to precisely determine the energy of the machine when the three measurements are taken is crucial for the success of the three-point technique. A mis-determination of the *spacing* of the measurements by just 3% would result in an error in  $\Gamma_{h_{SM}}^{\text{tot}}$  of 30%. This does not present a problem provided some polarization of the beam can be achieved so that the precession of the spin of the muon as it circulates in the final storage ring can be measured. Given this and the rotation rate, the energy can be determined to the nearly 1 part in a million accuracy required. This energy calibration capability must be incorporated in the machine design from the beginning.

The other quantity that can be measured with great precision at a  $\mu^+\mu^-$  collider for a SM-like Higgs with  $m_h \lesssim 130 \text{ GeV}$  is  $G(b\bar{b}) \equiv \Gamma(h \rightarrow \mu^+\mu^-)BF(h \rightarrow b\bar{b})$ . For  $L = 50 \text{ fb}^{-1}$  and  $R = 0.01\%, 0.06\%$ ,  $G(b\bar{b})$  can be measured with an accuracy of  $\pm 0.4\%, \pm 2\%$  ( $\pm 3\%, \pm 15\%$ ) at  $m_h = 110 \text{ GeV}$  ( $m_h = m_Z$ ). By combining this measurement with the  $\pm \sim 7\%$  determination of  $BF(h \rightarrow b\bar{b})$  that could be made in the  $Zh$  production mode, a roughly  $\pm 8 - 10\%$  determination of  $\Gamma(h \rightarrow \mu^+\mu^-)$  becomes possible. ( $R = 0.01\%$  is required if  $m_h \sim m_Z$ .)

Suppose we find a light Higgs  $h$  and measure its mass, total width and partial widths. The critical questions that then arise are:

- Can we determine if the particle is a SM Higgs or a supersymmetric Higgs?
- If the particle is a supersymmetric Higgs boson, say in the MSSM, can we then predict masses of the heavier Higgs bosons  $H^0$ ,  $A^0$ , and  $H^\pm$  in order to discover them in subsequent measurements?

In the context of the MSSM, the answers to these questions can be delineated.

Although enhancements of  $\Gamma_h^{\text{tot}}$  of order 30% relative to the prediction for the SM  $h_{SM}$  are the norm (even neglecting possible SUSY decays) for  $m_{A^0} \lesssim 400 \text{ GeV}$ , the possibilities of stop mixing and/or SUSY decays would not allow unambiguous interpretation and determination of  $m_{A^0}$ . However, and here is the crucial point,  $\Gamma_h^{\text{tot}}$  could be combined with branching ratios to yield a fairly definitive determination of  $m_{A^0}$ . For instance, we can compute  $\Gamma(h \rightarrow b\bar{b}) = \Gamma_h^{\text{tot}} BF(h \rightarrow b\bar{b})$  using  $BF(h \rightarrow b\bar{b})$  as measured in  $Zh$  production. It turns out that the percentage deviation of this



partial width for the  $h^0$  from the  $h_{SM}$  prediction is rather independent of  $\tan\beta$  and gives a mixing-independent determination of  $m_{A^0}$ , which, after including systematic uncertainties in our knowledge of  $m_b$ , would discriminate between a value of  $m_{A^0} \leq 300$  GeV vs.  $m_{A^0} = \infty$  at the  $\geq 3\sigma$  statistical level.

Returning to  $\Gamma(h \rightarrow \mu^+\mu^-)$ , deviations at the  $\gtrsim 3\sigma$  statistical level in the prediction for this partial width for the  $h^0$  as compared to the  $h_{SM}$  are predicted out to  $m_{A^0} \gtrsim 400$  GeV. Further, the percentage of deviation from the SM prediction would provide a relatively accurate determination of  $m_{A^0}$  for  $m_{A^0} \lesssim 400$  GeV. For example, if  $m_h = 110$  GeV,  $\Gamma(h^0 \rightarrow \mu^+\mu^-)$  changes by 20% (a  $\gtrsim 2\sigma$  effect) as  $m_{A^0}$  is changed from 300 GeV to 365 GeV.

Deviations for compound quantities, e.g.  $BF(h \rightarrow b\bar{b})$  defined by the ratio  $\Gamma(h \rightarrow b\bar{b})/\Gamma_h^{\text{tot}}$ , depend upon the details of the stop squark masses and mixings, the presence of SUSY decay modes, and so forth, much as described in the case of  $\Gamma_h^{\text{tot}}$ . Only partial widths yield a mixing-independent determination of  $m_{A^0}$ . The  $\mu^+\mu^-$  collider provides, as described, at least two particularly unique opportunities for determining two very important partial widths,  $\Gamma(h \rightarrow b\bar{b})$  and  $\Gamma(h \rightarrow \mu^+\mu^-)$ , thereby allowing a test of the predicted proportionality of these partial widths to fermion mass independent of the lepton/quark nature of the fermion.

Thus, if  $m_{A^0} \lesssim 400$  GeV, we may gain some knowledge of  $m_{A^0}$  through precision measurements of the  $h^0$ 's partial widths. This would greatly facilitate direct observation of the  $A^0$  and  $H^0$  via  $s$ -channel production at a  $\mu^+\mu^-$  collider with  $\sqrt{s} \lesssim 500$  GeV. As discussed in more detail shortly, even without such pre-knowledge of  $m_{A^0}$ , discovery of the  $A^0, H^0$  Higgs bosons would be possible in the  $s$ -channel at a  $\mu^+\mu^-$  collider provided that  $\tan\beta \gtrsim 3-4$ . With pre-knowledge of  $m_{A^0}$ , detection becomes possible for  $\tan\beta$  values not far above 1, provided  $R \sim 0.01\%$  (crucial since the  $A^0$  and  $H^0$  become relatively narrow for low  $\tan\beta$  values).

Other colliders offer various mechanisms to directly search for the  $A^0, H^0$ , but also have limitations:

- The LHC has a discovery hole and “ $h^0$ -only” regions at moderate  $\tan\beta$ ,  $m_{A^0} \gtrsim 200$  GeV.
- At the NLC one can use the mode  $e^+e^- \rightarrow Z^* \rightarrow H^0 A^0$  (the mode  $h^0 A^0$  is suppressed for large  $m_{A^0}$ ), but it is limited to  $m_{H^0} \sim m_{A^0} \lesssim \sqrt{s}/2$ .
- A  $\gamma\gamma$  collider could probe heavy Higgs up to masses of  $m_{H^0} \sim m_{A^0} \sim 0.8\sqrt{s}$ , but this would quite likely require  $L \sim 100 \text{ fb}^{-1}$ , especially if the Higgs bosons are at the upper end of the  $\gamma\gamma$  collider energy spectrum [21].

Since most GUT models predict  $m_{A^0} \gtrsim 200$  GeV, and perhaps as large as a TeV, the ability to search up to  $m_{A^0} \sim m_{H^0} \sim \sqrt{s}$  in the  $s$ -channel is a clear advantage of a  $\mu^+\mu^-$  collider. For example, at a muon collider with  $\sqrt{s} \sim 500$  GeV and with  $L = 50 \text{ fb}^{-1}$ , scan detection of the  $A^0, H^0$  is possible in the mass range from 200 to 500 GeV in  $s$ -channel production, provided  $\tan\beta \gtrsim 3-4$ , whereas an  $e^+e^-$  collider of the same energy can only probe  $m_{H^0} \sim m_{A^0} \lesssim 220$  GeV. That the signals become viable

when  $\tan\beta > 1$  (as favored by GUT models) is due to the fact that the couplings of  $A^0$  and (once  $m_{A^0} \gtrsim 150$  GeV)  $H^0$  to  $b\bar{b}$  and, especially to  $\mu^+\mu^-$ , are proportional to  $\tan\beta$ , and thus increasingly enhanced as  $\tan\beta$  rises.

Although the  $H^0, A^0$  cannot be discovered for  $\tan\beta \lesssim 3$  if one must scan the entire 200 – 500 GeV range, this is a range in which the LHC *could* find the heavy Higgs bosons in a number of modes. That the LHC and the NMC are complementary in this respect is a very crucial point. Together, discovery of the  $A^0, H^0$  is essentially guaranteed.

If the  $H^0, A^0$  are observed at the  $\mu^+\mu^-$  collider, measurement of their widths will typically be straightforward. For moderate  $\tan\beta$  the  $A^0$  and  $H^0$  resonance peaks do not overlap and  $R \lesssim 0.06\%$  will be adequate, since for such  $R$  values  $\Gamma_{H^0, A^0} \gtrsim \sigma_{\sqrt{s}}$ . However, if  $\tan\beta$  is large, then for most of the  $m_{A^0} \gtrsim 200$  GeV parameter range the  $A^0$  and  $H^0$  are sufficiently degenerate that there is significant overlap of the  $A^0$  and  $H^0$  resonance peaks. In this case,  $R \sim 0.01\%$  resolution would be necessary for observing the double-peaked structure and separating the  $A^0$  and  $H^0$  resonances.

A  $\sqrt{s} \sim 500$  GeV muon collider still might not have sufficient energy to discover heavy supersymmetric Higgs bosons. Further, distinguishing the MSSM from the SM by detecting small deviations of the  $h^0$  properties from those predicted for the  $h_{SM}$  becomes quite difficult for  $m_{A^0} \gtrsim 400$  GeV. However, construction of a higher energy machine, say  $\sqrt{s} = 4$  TeV, would allow discovery of  $\mu^+\mu^- \rightarrow A^0 H^0$  pair production via the  $b\bar{b}$  or  $t\bar{t}$  decay channels of the  $H^0, A^0$  (see the discussion in Section 5).

We close this section with brief comments on the effects of bremsstrahlung and beam polarization. Soft photon radiation must be included when determining the resolution in energy and the peak luminosity achievable at an  $e^+e^-$  or  $\mu^+\mu^-$  collider. This radiation is substantially reduced at a  $\mu^+\mu^-$  collider due to the increased mass of the muon compared to the electron. The bremsstrahlung effects are calculated in Ref. [17].

For a SM-like Higgs boson with  $\Gamma_h^{\text{tot}} < \sigma_{\sqrt{s}}$ , the primary effect of bremsstrahlung arises from the reduction in the luminosity at the Gaussian peak which results in the same percentage reduction in the maximum achievable Higgs production rate. The conclusions above regarding  $s$ -channel Higgs detection are those obtained with inclusion of bremsstrahlung effects.

Although reduced in magnitude compared to an electron collider, there is a long low-energy bremsstrahlung tail at a muon collider that provides a self-scan over the range of energies below the design energy, and thus can be used to detect  $s$ -channel resonances. Observation of  $A^0, H^0$  peaks in the  $b\bar{b}$  mass distribution  $m_{b\bar{b}}$  created by this bremsstrahlung tail may be possible. The region of the  $(m_{A^0}, \tan\beta)$  parameter space plane for which a peak is observable depends strongly on the  $b\bar{b}$  invariant mass resolution. For an excellent  $m_{b\bar{b}}$  mass resolution of order  $\pm 5$  GeV and integrated luminosity of  $L = 50 \text{ fb}^{-1}$  at  $\sqrt{s} = 500$  GeV, the  $A^0, H^0$  peak(s) are observable for  $\tan\beta \gtrsim 5$  at  $m_{A^0} \gtrsim 400$  GeV (but only for very large  $\tan\beta$  values in the  $m_{A^0} \sim m_Z$  region due to the large  $s$ -channel  $Z$  contribution to the  $b\bar{b}$  background).

In the  $s$ -channel Higgs studies, polarization of the muon beams could present

a significant advantage over the unpolarized case, since signal and background come predominantly from different polarization states. Polarization  $P$  of both beams would enhance the significance of a Higgs signal provided the factor by which the luminosity is reduced is not larger than  $(1+P^2)^2/(1-P^2)$ . For example, a reduction in luminosity by a factor of 10 could be compensated by a polarization  $P = 0.84$ , leaving the significance of the signal unchanged [22]. Furthermore, *transverse* polarization of the muon beams could prove useful for studying CP-violation in the Higgs sector. Muons are produced naturally polarized from  $\pi$  and  $K$  decays. An important consideration for the future design of muon colliders is the extent to which polarization can be maintained through the cooling and acceleration processes.

### 3 Precision Threshold Studies

Good beam energy resolution is crucial for the determination of the Higgs width. Another area of physics where the naturally good resolution of a  $\mu^+\mu^-$  collider would prove valuable is studies of the  $t\bar{t}$  and  $W^+W^-$  thresholds, similar to those proposed for the NLC and LEP II. The  $t\bar{t}$  threshold shape determines  $m_t$ ,  $\Gamma_t$  and the strong coupling  $\alpha_s$ , while the  $W^+W^-$  threshold shape determines  $m_W$  and possibly also  $\Gamma_W$ . At a  $\mu^+\mu^-$  collider, even a conservative natural beam resolution  $R \sim 0.1\%$  would allow substantially increased precision in the measurement of most of these quantities as compared to other machines. Not only is such monochromaticity already greatly superior to  $e^+e^-$  collider designs, where typically  $R \sim 1\%$ , but also at a  $\mu^+\mu^-$  collider there is no significant beamstrahlung and the amount of initial state radiation (ISR) is greatly reduced. ISR and, especially, beam smearing cause significant loss of precision in the measurement of the top quark and  $W$  masses at  $e^+e^-$  colliders.

To illustrate, consider threshold production of the top quark, which has been extensively studied for  $e^+e^-$  colliders [24]. Figure 4 shows the effects of including beam smearing and ISR for the threshold production of top quarks using a Gaussian beam spread of 1% for the  $e^+e^-$  collider. Also shown are our corresponding results for the  $\mu^+\mu^-$  collider with  $R = 0.1\%$  as presented in Ref. [25]. The threshold peak is no longer washed out in the  $\mu^+\mu^-$  case. The precision with which one could measure  $m_t$ ,  $\alpha_s$  and  $\Gamma_t$  at various facilities is shown in Table 1. Improvements in the determination of  $m_W$  should also be possible [23].

The value of such improvements in precision can be substantial. Consider precision electroweak corrections, for example. The prediction for the SM or SM-like Higgs mass  $m_h$  depends on  $m_W$  and  $m_t$  through the one-loop equation

$$m_W^2 = m_Z^2 \left[ 1 - \frac{\pi\alpha}{\sqrt{2}G_\mu m_W^2(1 - \delta r)} \right]^{1/2}, \quad (12)$$

where  $\delta r$  depends quadratically on  $m_t$  and logarithmically on  $m_h$ . Current expectations for LEP II and the Tevatron imply precisions of order

$$\Delta m_W = 40 \text{ MeV} , \quad \Delta m_t = 4 \text{ GeV} . \quad (13)$$

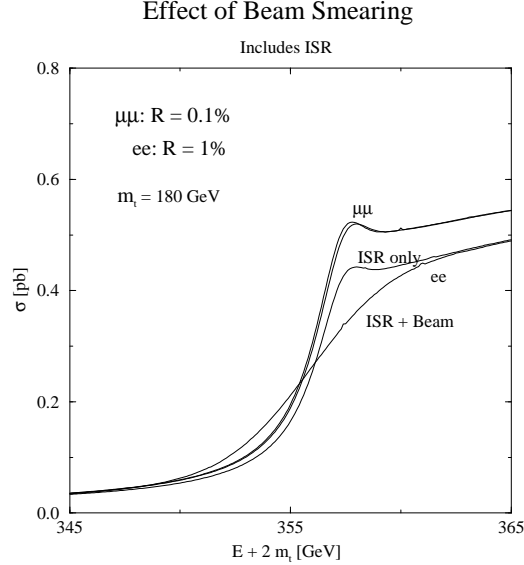


Figure 4: The threshold curves are shown for  $\mu^+\mu^-$  and  $e^+e^-$  machines including ISR and with and without beam smearing. Beam smearing has only a small effect at a muon collider, whereas at an electron collider the threshold region is significantly smeared. The strong coupling is taken to be  $\alpha_s(m_Z) = 0.12$ .

For the uncertainties of Eq. (13) and the current central values of  $m_W = 80.4$  GeV and  $m_t = 180$  GeV, the Higgs mass would be constrained to the  $1\sigma$  range

$$50 < m_h < 200 \text{ GeV} . \quad (14)$$

In electroweak precision analyses, an error of  $\Delta m_W = 40$  MeV is equivalent to an error of  $\Delta m_t = 6$  GeV, so increased precision for  $m_W$  would be of greatest immediate interest given the  $\Delta m_t = 4$  GeV error quoted above. In order to make full use of the  $\Delta m_t \lesssim 0.5$  GeV precision possible at a  $\mu^+\mu^-$  collider would require  $\Delta m_W \lesssim 4$  MeV. We are currently studying the possibility that the latter can be achieved at a  $\mu^+\mu^-$  collider.

Such precisions, combined with the essentially exact determination of  $m_h$  possible at a  $\mu^+\mu^-$  collider, would allow a consistency test for precision electroweak measurements at a hitherto unimagined level of accuracy. If significant inconsistency is found, new physics could be revealed. For example, inconsistency could arise if the light  $h$  is not that of the SM but rather the  $h^0$  of the MSSM and there is a contribution to precision electroweak quantities arising from the  $H^0$  of the MSSM having a non-negligible  $WW$ ,  $ZZ$  coupling. The contributions of stop and chargino states to loops would be another example.

A precise determination of the top quark mass  $m_t$  could well be important in its own right. For instance, in GUT scenarios  $m_t$  determines to a large extent the

Table 1: Measurements of the standard model parameters: top mass  $m_t$ , strong coupling  $\alpha_s$ , and top quark width  $\Gamma_t$ .

	Tevatron (1000 $pb^{-1}$ ) (10 $fb^{-1}$ )	LHC (20 $pb^{-1}$ )	NLC (10 $fb^{-1}$ )	FMC (10 $fb^{-1}$ )
$\Delta m_t(\text{GeV})$	4 1	2	0.52[26]	0.3
$\Delta\alpha_s$			0.009	0.008
$\Delta\Gamma_t/\Gamma_t$	0.3[27]		0.2	better

evolution of all the other Yukawas, including flavor mixings. If the top quark Yukawa coupling is determined by an infrared quasi-fixed point, very small changes in the top quark mass translate into very large changes in the renormalized values of many other parameters in the theory.

## 4 CP violation and FCNC in the Higgs Sector

A nonstandard Higgs sector could have sizable CP-violating effects as well as new flavor changing neutral current (FCNC) effects that could be probed with a  $\mu^+\mu^-$  collider. A general two Higgs doublet model has been studied in Refs. [29,30,31]. There one would either (i) measure correlations in the final state, or (ii) transversely polarize the muon beams to observe an asymmetry in the production rate as a function of spin orientation. For the second option, the ability to achieve transverse polarization with the necessary luminosity is a crucial consideration.

New FCNC effects could be studied as well [32]. For example a Higgs in the  $s$ -channel could exhibit the decay  $\mu^+\mu^- \rightarrow H^0 \rightarrow t\bar{c}$ . This decay would have to compete against the  $WW^*$  decays.

## 5 Exotic Higgs Bosons/Scalars

In general, a muon collider can probe any type of scalar that has significant fermionic couplings. Interesting new physics could be revealed. To give one example, consider the possibility that a doubly-charged Higgs boson with lepton-number-violating coupling  $\Delta^{--} \rightarrow \ell^-\ell^-$  exists, as required in left-right symmetric models where the neutrino mass is generated by the see-saw mechanism through a vacuum expectation value of a neutral Higgs triplet field. Such a  $\Delta^{--}$  could be produced in  $\ell^-\ell^-$  collisions. This scenario was studied in Ref. [33] for an  $e^-e^-$  collider, but a  $\mu^-\mu^-$  collider would be even better due to the much finer energy resolution (which

enhances cross sections) and the fact that the  $\Delta^{--} \rightarrow \mu^- \mu^-$  coupling should be larger than the  $\Delta^{--} \rightarrow e^- e^-$  coupling.

Most likely, a  $\Delta^{--}$  in the  $\lesssim 500$  GeV region would already be observed at the LHC by the time the muon collider begins operation. In some scenarios, it would even be observed to decay to  $\mu^- \mu^-$  so that the required  $s$ -channel coupling would be known to be non-zero. However, the magnitude of the coupling would not be determined; for this we would need the  $\mu^- \mu^-$  collider. In the likely limit where  $\Gamma_{\Delta^{--}} \ll \sigma_{\sqrt{s}}$ , the number of  $\Delta^{--}$  events for  $L = 50 \text{ fb}^{-1}$  is given by

$$N(\Delta^{--}) = 6 \times 10^{11} \left( \frac{c_{\mu\mu}}{10^{-5}} \right) \left( \frac{0.01\%}{R(\%)} \right), \quad (15)$$

where the standard Majorana-like coupling-squared is parameterized as

$$|h_{\mu\mu}|^2 = c_{\mu\mu} m_{\Delta^{--}}^2 (\text{GeV}). \quad (16)$$

Current limits on the coupling correspond to  $c_{\mu\mu} \lesssim 5 \times 10^{-5}$ . Assuming that 30 to 300 events would provide a distinct signal (the larger number probably required if the dominant  $\Delta^{--}$  decay channel is into  $\mu^- \mu^-$ , for which there is a significant  $\mu^- \mu^- \rightarrow \mu^- \mu^-$  background), the muon collider would probe some 11 to 10 orders of magnitude more deeply in the coupling-squared than presently possible. This is a level of sensitivity that would almost certainly be adequate for observing a  $\Delta^{--}$  that is associated with the triplet Higgs boson fields that give rise to see-saw neutrino mass generation in the left-right symmetric models.

## 6 Physics at a $2 \otimes 2$ TeV $\mu^+ \mu^-$ Collider

Bremsstrahlung radiation scales like  $m^{-4}$ , so a circular storage ring can be used for muons at high energies. A high energy lepton collider with center-of-mass energy of 4 TeV would provide new physics reach beyond that contemplated at the LHC or NLC (with  $\sqrt{s} \lesssim 1.5$  TeV). We concentrate primarily on the following scenarios for physics at these energies: (1) heavy supersymmetric (SUSY) particles, (2) strong scattering of longitudinal gauge bosons (generically denoted  $V_L$ ) in the electroweak symmetry breaking (EWSB) sector, and (3) heavy vector resonance production, like a  $Z'$ .

### 6.1 SUSY Factory

Low-energy supersymmetry is a theoretically attractive extension of the Standard Model. Not only does it solve the naturalness problem, but also the physics remains essentially perturbative up to the grand unification scale, and gravity can be included by making the supersymmetry local. Since the SUSY-breaking scale and, hence, sparticle masses are required by naturalness to be no larger than 1 – 2 TeV, a high

energy  $\mu^+\mu^-$  collider with  $\sqrt{s} = 4$  TeV is guaranteed to be a SUSY factory if SUSY is nature's choice. Indeed, it may be the only machine that would guarantee our ability to study the full spectrum of SUSY particles. The LHC has sufficient energy to produce supersymmetric particles but disentangling the spectrum and measuring the masses will be a challenge due to the complex cascade decays and QCD backgrounds. The NLC would be a cleaner environment than the LHC to study the supersymmetric particle decays, but the problem here may be insufficient energy to completely explore the full particle spectrum.

Most supersymmetric models have a symmetry known as an  $R$ -parity that requires that supersymmetric particles be created or destroyed in pairs. This means that the energy required to find and study heavy scalars is more than twice their mass. (If  $R$ -parity is violated, then sparticles can also be produced singly; the single sparticle production rate would depend on the magnitude of the violation, which is model- and generation-dependent.) Further, a  $p$ -wave suppression is operative for the production of scalars (in this case the superpartners to the ordinary quarks and leptons), and energies well above the kinematic threshold might be required to produce the scalar pairs at an observable rate. In addition, a large lever arm for exploring the different threshold behaviour of spin-0 and spin-1/2 SUSY particles could prove useful in mass determinations.

To be more specific, it is useful to constrain the parameter space by employing a supergravity (SUGRA) model. A model which illustrates the potential of the muon collider, while obeying all known constraints, including those arising from naturalness and the need for cold dark matter in the universe, is detailed in Ref. [11]. In this model, the scalars are heavy (with the exception of the lightest Higgs boson) compared to the gauginos. The particle and sparticle masses obtained from renormalization group evolution are:

$$\begin{aligned} m_{h^0} &= 88 \text{ GeV}, & m_{A^0} &= 921 \text{ GeV}, & m_{H^\pm} &= m_{H^0} = 924 \text{ GeV}, \\ m_{\tilde{q}_L} &\simeq 752 \text{ GeV}, & m_{\tilde{q}_R} &\simeq 735 \text{ GeV}, & m_{\tilde{b}_1} &= 643 \text{ GeV}, & m_{\tilde{b}_2} &= 735 \text{ GeV}, \\ m_{\tilde{t}_1} &= 510 \text{ GeV}, & m_{\tilde{t}_2} &= 666 \text{ GeV}, & m_{\tilde{\nu}} &\sim m_{\tilde{\ell}} \sim 510 - 530 \text{ GeV}, \\ m_{\tilde{\chi}_{1,2,3,4}^0} &= 107, 217, 605, 613 \text{ GeV}, & m_{\tilde{\chi}_{1,2}^\pm} &= 217, 612 \text{ GeV}. \end{aligned}$$

Thus, we have a scenario such that pair production of heavy scalars is only accessible at a high energy machine like the NMC.

First, we consider the pair production of the heavy Higgs bosons

$$\mu^+\mu^- \rightarrow Z \rightarrow H^0 A^0, \quad (17)$$

$$\mu^+\mu^- \rightarrow \gamma, Z \rightarrow H^+ H^-. \quad (18)$$

The cross sections are shown in Fig. 5 versus  $\sqrt{s}$ . A  $\mu^+\mu^-$  collider with  $\sqrt{s} \gtrsim 2$  TeV is needed and well above the threshold the cross section is  $\mathcal{O}(1 \text{ fb})$ . In the current scenario, the decays of these heavy Higgs bosons are predominantly into top quark modes ( $t\bar{t}$  for the neutral Higgs and  $t\bar{b}$  for the charged Higgs), with branching fractions near 90%. Observation of the  $H^0$ ,  $A^0$ , and  $H^\pm$  would be straightforward even for a

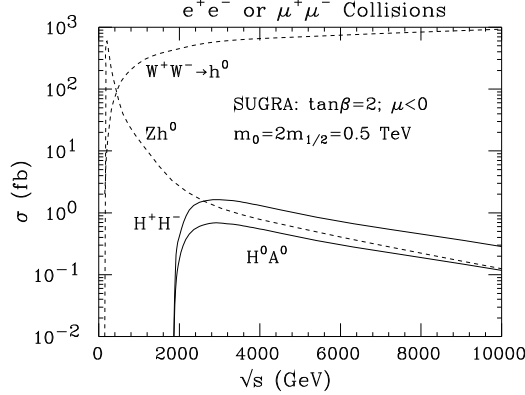


Figure 5: Pair production of heavy Higgs bosons at a high energy lepton collider. For comparison, cross sections for production of the lightest Higgs boson via the Bjorken process  $\mu^+\mu^- \rightarrow Z^* \rightarrow Zh^0$  and via  $WW$  fusion are also presented.

pessimistic luminosity of  $L = 100 \text{ fb}^{-1}$ . Backgrounds would be negligible once the requirement of roughly equal masses for two back-to-back particles is imposed.

In other scenarios the decays may be more complex and include multiple decay modes into supersymmetric particles, in which case the overall event rate might prove crucial to establishing a signal. In some scenarios investigated in Ref. [34] complex decays are important, but the  $\mu^+\mu^-$  collider has sufficient production rate that one or more of the modes

$$(H^0 \rightarrow b\bar{b}) + (A^0 \rightarrow b\bar{b}) , \quad (19)$$

$$(H^0 \rightarrow h^0 h^0 \rightarrow b\bar{b}b\bar{b}) + (A^0 \rightarrow X) , \quad (20)$$

$$(H^0 \rightarrow t\bar{t}) + (A^0 \rightarrow t\bar{t}) , \quad (21)$$

are still visible above the backgrounds for  $L \gtrsim 500 \text{ fb}^{-1}$ . Despite the significant dilution of the signal by the additional SUSY decay modes (which is most important at low  $\tan\beta$ ), one can observe a signal of  $\gtrsim 50$  events in one channel or another.

The high energy  $\mu^+\mu^-$  collider will yield a large number of the light SM-like  $h^0$  via  $\mu^+\mu^- \rightarrow Z^* \rightarrow Zh^0$  and  $WW$  fusion,  $\mu^+\mu^- \rightarrow \nu\bar{\nu}h^0$ . In contrast to a machine running at FMC energies ( $\sqrt{s} \sim 500 \text{ GeV}$ ), where the cross sections for these two processes are comparable, at higher energies,  $\sqrt{s} \gtrsim 1 \text{ TeV}$ , the  $WW$  fusion process dominates as shown in Fig. 5.

Any assessment of the physics signals in the pair production of the supersymmetric partners of the quarks and leptons is model-dependent. However, the present scenario is typical in that squarks are expected to be somewhat heavier than the sleptons due to their QCD interactions which affect the running of their associated ‘soft’ masses. Except for the LSP, the lightest superpartner of each type decays to a gaugino (or gluino) and an ordinary fermion, and the gaugino will decay if it is not the LSP. Since



the particles are generally too short-lived to be observed, we must infer everything about their production from their decay products.

We illustrate the production cross sections for several important sparticle pairs in Fig. 6 for the SUGRA model being considered. For a collider with  $\sqrt{s} \sim 4$  TeV, cross sections of  $\sim 2\text{--}30$  fb are expected.

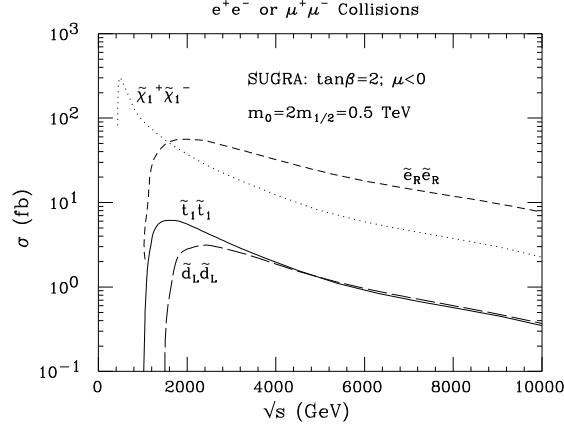


Figure 6: The production cross sections for SUSY particles in a supergravity model with heavy scalars.

The final states of interest are determined by the dominant decay modes, which in this model are  $\tilde{e}_R \rightarrow e\tilde{\chi}_1^0$  ( $BF = 0.999$ ),  $\tilde{\chi}_1^+ \rightarrow W^+\tilde{\chi}_1^0$  ( $BF = 0.999$ ),  $\tilde{d}_L \rightarrow \tilde{\chi}_1^- u, \tilde{\chi}_2^0 d, \tilde{g}d$  ( $BF = 0.52, 0.27, 0.20$ ), and  $\tilde{t}_1 \rightarrow \tilde{\chi}_1^+ t$ . Thus, for example, with a luminosity of  $L = 200 \text{ fb}^{-1}$  at  $\sqrt{s} = 4$  TeV,  $\tilde{d}_L$  pair production would result in  $200 \times 2 \times (0.52)^2 = 100$  events containing two  $u$ -quark jets, two energetic leptons (not necessarily of the same type), and substantial missing energy. The SM background should be small, and the signal would be clearly visible. The energy spectra of the quark jets would allow a determination of  $m_{\tilde{d}_L} - m_{\tilde{\chi}_1^+}$  while the lepton energy spectra would fix  $m_{\tilde{\chi}_1^+} - m_{\tilde{\chi}_1^0}$ . If the machine energy can be varied, then the turn-on of such events would fix the  $\tilde{d}_L$  mass. The  $\tilde{\chi}_1^+$  and  $\tilde{\chi}_1^0$  masses would presumably already be known from studying the  $\ell^+\ell^-$ +missing-energy signal from  $\tilde{\chi}_1^+\tilde{\chi}_1^-$  pair production, best performed at much lower energies. Thus, cross checks on the gaugino masses are possible, while at the same time two determinations of the  $\tilde{d}_L$  mass become available (one from threshold location and the other via the quark jet spectra combined with a known mass for the  $\tilde{\chi}_1^+$ ).

This example illustrates the power of a  $\mu^+\mu^-$  collider, especially one whose energy can be varied over a broad range. Maintaining high luminosity over a broad energy range may require the construction of several (relatively inexpensive) final storage rings.

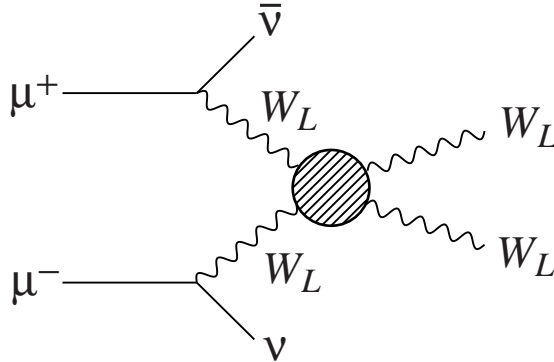


Figure 7: Symbolic diagram for strong WW scattering.

## 6.2 The $V_L V_L \rightarrow V_L V_L$ Probe of EWSB

Despite the extraordinary success of the Standard Model (SM) in describing particle physics up to the highest energy available today, the nature of electroweak symmetry-breaking (EWSB) remains undetermined. In particular, it is entirely possible that there is no light ( $\lesssim 700$  GeV) Higgs boson. General arguments based on partial wave unitarity then imply that the  $W^\pm, Z$  electroweak gauge bosons develop strong (non-perturbative) interactions by energy scales of order 1–2 TeV. For a collider to probe such energy scales, it must have sufficient energy that gauge-boson scattering (see Fig. 7) at subprocess energies at or above 1 TeV occurs with substantial frequency. Of the colliders under construction or being planned that potentially meet this requirement, a high energy muon-muon collider (NMC) would be the most optimal.

Our ability to extract signals and learn about a strongly-interacting-electroweak sector (SEWS) at the LHC and NLC has been the subject of many studies; see *e.g.* [36,37]. In general, the conclusion is that the LHC and NLC will yield first evidence for a SEWS theory, but that in many models the evidence will be weak and of rather marginal statistical significance. Models yielding large signals (*e.g.* a techni-rho resonance peak) will be readily apparent or easily eliminated, but the many models that result in only handfuls of excess events will be very difficult to distinguish from one another. And, certainly, for such models an actual measurement of the  $VV$  mass spectrum (here we generically denote  $W^\pm, Z$  by  $V$ ), which would reveal a wealth of information about the model, is completely out of the question. In contrast, a muon collider with center-of-mass energy,  $\sqrt{s}$ , of order 4 TeV would be in a fairly optimal energy range. It could provide a rather full and comprehensive study of the  $M_{VV}$  distributions in all channels, assuming (as should be the case) that  $\mu^+\mu^-$  and  $\mu^+\mu^+$  (or  $\mu^-\mu^-$ ) collisions are possible at the planned luminosity of  $L \sim 200 - 1000 \text{ fb}^{-1}$  per year. Construction of a multi-TeV  $e^+e^-$  collider might also be a possibility [38],

and would provide similar capabilities if an  $e^-e^-$  facility is included, although certain backgrounds would be larger.

In order to isolate the SEWS signals, it is necessary to determine if there are events in the  $\nu\bar{\nu}VV$  final states at large  $M_{VV}$  due to strong scattering of  $V$ 's with longitudinal ( $L$ ) polarization beyond those that will inevitably be present due to standard electroweak processes, including scattering, that produce  $V$ 's with transverse ( $T$ ) polarization. There are two obvious ways of determining if such events are present.

- The first is to look for the strong scattering events as an excess of events beyond what would be expected in the Standard Model if there is no strong scattering. This involves reliably computing the irreducible and reducible SM ‘backgrounds’ and subtracting from the total observed SEWS rate.
- The second is to employ projection techniques to independently isolate the  $V_LV_L$ ,  $V_TV_T$  and  $V_TV_L$  rates.

In this overview, extracted from Ref. [39], I only discuss the first technique. However, the projection technique also appears to be highly feasible at a muon collider operating at the full  $L = 1000 \text{ fb}^{-1}$  yearly luminosity.

Only the subtraction procedure is practical at the LHC and NLC (with  $\sqrt{s} \lesssim 1.5 \text{ TeV}$ ) because of limited event rates. In this procedure, the Standard Model with a light Higgs boson ( $h_{SM}$ ) is used to define the  $V_TV_T$  background. This is appropriate since when  $m_{h_{SM}}$  is small the  $VV$  final state is entirely  $V_TV_T$ , and since the  $V_TV_T$  rate is essentially independent of  $m_{h_{SM}}$ . As  $m_{h_{SM}}$  is increased, the entire growth in the  $VV$  cross section derives from the increasing strength of the interactions of longitudinally polarized  $V$ 's. The light Higgs SM is conventionally denoted as the “ $m_{h_{SM}} = 0$ ” model, although in practice we use  $m_{h_{SM}} = 10 \text{ GeV}$ . Thus, the SEWS signal is given by

$$\frac{d\Delta\sigma(SEWS)}{dM_{VV}} \equiv \frac{d\sigma(SEWS)}{dM_{VV}} - \frac{d\sigma(m_{h_{SM}} = 10 \text{ GeV})}{dM_{VV}}, \quad (22)$$

with  $\Delta\sigma(SEWS)$  being the integral thereof over a specified range of  $M_{VV}$ .

For a first estimate of the strong electroweak scattering effects we use the Standard Model with a heavy Higgs as a prototype of the strong scattering sector. For a 1 TeV SM Higgs boson, the SEWS signal is thus defined as

$$\Delta\sigma = \sigma(m_{h_{SM}} = 1 \text{ TeV}) - \sigma(m_{h_{SM}} = 10 \text{ GeV}). \quad (23)$$

Results for  $\Delta\sigma$  (with no cuts of any kind) are shown in Table 2 for  $\sqrt{s} = 1.5 \text{ TeV}$  (possibly the upper limit for an  $e^+e^-$  collider using current designs) and 4 TeV. The strong scattering signal is relatively small at energies of order 1 TeV, but grows substantially as multi-TeV energies are reached. The associated signal ( $S$ ) and background ( $B$ ) event rates are also given in Table 2. We see that at 4 TeV a very respectable signal rate is achieved and that even before cuts the signal to irreducible background ( $S/B$ ) ratio is quite reasonable; both are certainly much better than at

$\sqrt{s} = 1.5$  TeV. SEWS physics benefits from increasing energy both because the luminosities at higher energies are normally designed to be larger (to compensate for the decline of point-like cross sections behaving as  $1/s$ ) and because the (non-point-like) signal cross section and the signal/background ratio both increase. It appears that  $\sqrt{s} = 4$  TeV is roughly the critical energy at which SEWS physics can first be studied in detail. Thus, the highest energies in  $\sqrt{s}$  that can be reached at a muon collider could be critically important.

Table 2: Strong electroweak scattering signals in  $W^+W^- \rightarrow W^+W^-$  and  $W^+W^- \rightarrow ZZ$  at future lepton colliders. Signal cross sections and  $S/B$  values (for  $L = 200 \text{ fb}^{-1}$  at  $\sqrt{s} = 1.5$  TeV and  $L = 1000 \text{ fb}^{-1}$  at  $\sqrt{s} = 4$  TeV, with no cuts) are given.

$\sqrt{s}$	$\Delta\sigma(W^+W^-)$	$[S/B](W^+W^-)$	$\Delta\sigma(ZZ)$	$[S/B](ZZ)$
1.5 TeV	8 fb	$\frac{1600}{8000}$	6 fb	$\frac{1200}{3600}$
4 TeV	80 fb	$\frac{80000}{170000}$	50 fb	$\frac{50000}{80000}$

Many other models for the strongly interacting gauge sector have been constructed in addition to the SM. The additional models upon which we focus here are [36]:

- a (“Scalar”) model in which there is a scalar Higgs resonance with  $M_S = 1$  TeV but non-SM width of  $\Gamma_S = 350$  GeV;
- a (“Vector”) model in which there is no scalar resonance, but rather a vector resonance with either  $M_V = 1$  TeV and  $\Gamma_V = 35$  GeV or  $M_V = 2$  TeV and  $\Gamma_V = 0.2$  TeV.
- a model, denoted by LET-K or “ $m_{h_{SM}} = \infty$ ”, in which the SM Higgs is taken to have infinite mass and the partial waves simply follow the behavior predicted by the low-energy theorems, except that the LET behavior is unitarized via  $K$ -matrix techniques.

The  $I = 0, 1, 2$  weak-isospin amplitudes are each distinctly different for the different models, and the ultimate goal is to fully explore these different isospin channels in order to determine the model. The processes

$$\begin{aligned}
W^+W^- &\rightarrow W^+W^-, ZZ, \\
W^\pm Z &\rightarrow W^\pm Z, \\
W^\pm W^\pm &\rightarrow W^\pm W^\pm,
\end{aligned} \tag{24}$$

provide as much information as can be accessed experimentally. A 4 TeV muon collider can provide at least a reasonably good determination of the spectrum for each of the above reactions as a function of  $s = M_V^2$ . In contrast, for most models the LHC or a  $\sqrt{s} \lesssim 1.5$  TeV NLC can at best allow determination of integrals over broad ranges of  $M_V$ .

If the electroweak sector is strongly interacting, partial exploration of the model in the three weak-isospin channels ( $I = 0, 1, 2$ ) will be possible at the LHC. Discrimination between models is achieved by comparing the gold-plated purely-leptonic event rates in the different  $VV$  channels to one another. However, only in the case of the  $M_V = 1$  TeV Vector model would there be any chance of actually observing details regarding the structure of the  $M_{VV}$  spectrum. A  $M_V = 2$  TeV Vector model would be virtually indistinguishable from the LET-K model. These same channels have also been studied for a 1.5 TeV NLC [37], and, again, event rates are at a level that first signals of the strongly interacting vector boson sector would emerge, but the ability to discriminate between models and actually study the strong interactions through the  $M_{VV}$  distributions would be limited.

Table 3: Total numbers of  $W^+W^-$ ,  $ZZ$  and  $W^+W^+ \rightarrow 4\text{-jet}$  signal ( $S$ ) and background ( $B$ ) events calculated for a 4 TeV  $\mu^+\mu^-$  collider with integrated luminosity  $200 \text{ fb}^{-1}$  ( $1000 \text{ fb}^{-1}$  in the parentheses), for cuts of  $M_{VV} \geq 500 \text{ GeV}$ ,  $p_T(V) \geq 150 \text{ GeV}$ ,  $|\cos \theta_V| \leq 0.8$  and  $p_T(VV) \geq 30 \text{ GeV}$ . (For the case of a 2 TeV vector state, events for the  $W^+W^-$  channel are summed around the mass peak over the range  $1.7 < M_{VV} < 2.3 \text{ TeV}$ .) In addition, we veto events containing a  $\mu^+$  or  $\mu^-$  with  $\theta_\mu \geq 12^\circ$  and  $E_\mu \geq 50 \text{ GeV}$ . The signal rate  $S$  is that obtained by computing the total rate (including all backgrounds) for a given SEWS model and then subtracting the background rate; see Eq. (23). The statistical significance  $S/\sqrt{B}$  is also given. The hadronic branching fractions of  $VV$  decays and the  $W^\pm/Z$  identification/misidentification are included.

channels	Scalar $m_H = 1 \text{ TeV}$ $\Gamma_H = 0.5 \text{ TeV}$	Vector $M_V = 2 \text{ TeV}$ $\Gamma_V = 0.2 \text{ TeV}$	LET-K $m_{h_{SM}} = \infty$ Unitarized
$\mu^+\mu^- \rightarrow \bar{\nu}\nu W^+W^-$			
$S(\text{signal})$	2400 (12000)	180 (890)	370 (1800)
$B(\text{backgrounds})$	1200 (6100)	25 (120)	1200 (6100)
$S/\sqrt{B}$	68 (152)	36 (81)	11 (24)
$\mu^+\mu^- \rightarrow \bar{\nu}\nu ZZ$			
$S(\text{signal})$	1030 (5100)	360 (1800)	400 (2000)
$B(\text{backgrounds})$	160 (800)	160 (800)	160 (800)
$S/\sqrt{B}$	81 (180)	28 (64)	32 (71)
$\mu^+\mu^+ \rightarrow \bar{\nu}\bar{\nu} W^+W^+$			
$S(\text{signal})$	240 (1200)	530 (2500)	640 (3200)
$B(\text{backgrounds})$	1300 (6400)	1300 (6400)	1300 (6400)
$S/\sqrt{B}$	7 (15)	15 (33)	18 (40)

For a  $\mu^+\mu^-$  collider operating at 4 TeV the event rates and statistical significances for most channels are much larger. Table 3 summarizes results in the  $W^+W^- \rightarrow W^+W^-$ ,  $W^+W^- \rightarrow ZZ$  and  $W^+W^+ \rightarrow W^+W^+$  channels<sup>†</sup> for the total signal  $S$  and background  $B$  event numbers obtained (after cuts) by summing over diboson invariant mass bins as specified in the caption, together with the statistical significance  $S/\sqrt{B}$ , for different models of the strongly-interacting physics. The signal rate  $S$  is that obtained after subtracting the background rate  $B$  from the net event rate (signal+background) for a given SEWS model, see Eq. (23). The  $ZZ$  and  $WW$  channels have been separated from one another on a statistical basis by employing the four-jet final state and requiring that both  $jj$  masses are near  $m_Z$  and  $m_W$ , respectively. See Ref. [39] for details. The jet energy resolution required is consistent with the better current detector plans for the NLC and JLC.

The results of Table 3 are easily summarized. Most importantly, the statistical significance of the SEWS signal is high (often *very* high) for all channels, regardless of model. Models of distinctly different types will be easily distinguished from one another. A broad Higgs-like scalar will enhance both  $W^+W^-$  and  $ZZ$  channels with  $\sigma(W^+W^-) > \sigma(ZZ)$ ; a  $\rho$ -like vector resonance will manifest itself through  $W^+W^-$  but not  $ZZ$ ; the unitarized  $m_{h_{SM}} = \infty$  (LET-K) amplitude will enhance  $ZZ$  more than  $W^+W^-$ .

In Fig. 8 we compare the  $M_{VV}$  distributions in the  $W^+W^-$  and  $ZZ$  final states for the various SEWS models considered in Table 3 (including the combined reducible and irreducible backgrounds) to those for the combined background only, after imposing all the cuts listed in the caption to Table 3. SEWS models illustrated are the SM with  $m_{h_{SM}} = 1$  TeV, the unitarized  $m_{h_{SM}} = \infty$  (LET-K) model, and a Vector model with  $M_V = 2$  TeV and  $\Gamma_V = 0.2$  TeV. The integrals over the specified  $M_{VV}$  ranges are the results that were tabulated in Table 3, where the signal event numbers are those obtained after subtracting the background from the full SEWS model curves of these figures (which include the combined background). To indicate the accuracy with which the  $M_{VV}$  distributions could be measured, we have shown the  $L = 200 \text{ fb}^{-1}$ ,  $\pm\sqrt{N}$  error bars associated with several 40 GeV bins for the LET-K model.

From these plots and the sample error bars, it is apparent that for any of the SEWS models investigated the expected signal plus background could be readily distinguished from pure background alone on a bin by bin basis at better than  $1\sigma$  all the way out to  $M_{VV} = 2.5$  TeV (2 TeV) in the  $W^+W^-$  and  $W^+W^+$  ( $ZZ$ ) channels. Further, the small 2 TeV Vector model peak would be readily apparent in the  $W^+W^-$  channel and its absence in the  $ZZ$  and  $W^+W^+$  channels would be clear. Indeed, it would be feasible to determine the width of either a scalar or a vector resonance with moderate accuracy.

Currently discussed designs for the 4 TeV muon collider would actually provide luminosity of  $L = 1000 \text{ fb}^{-1}$  per year. Even if this goal is not reached, one might rea-

---

<sup>†</sup>We focus on the  $W^+W^+ \rightarrow W^+W^+$  like-sign channel, but exactly the same results would apply for the  $W^-W^- \rightarrow W^-W^-$  channel. However, high luminosity  $\mu^+\mu^+$  collisions may be slightly easier to achieve.

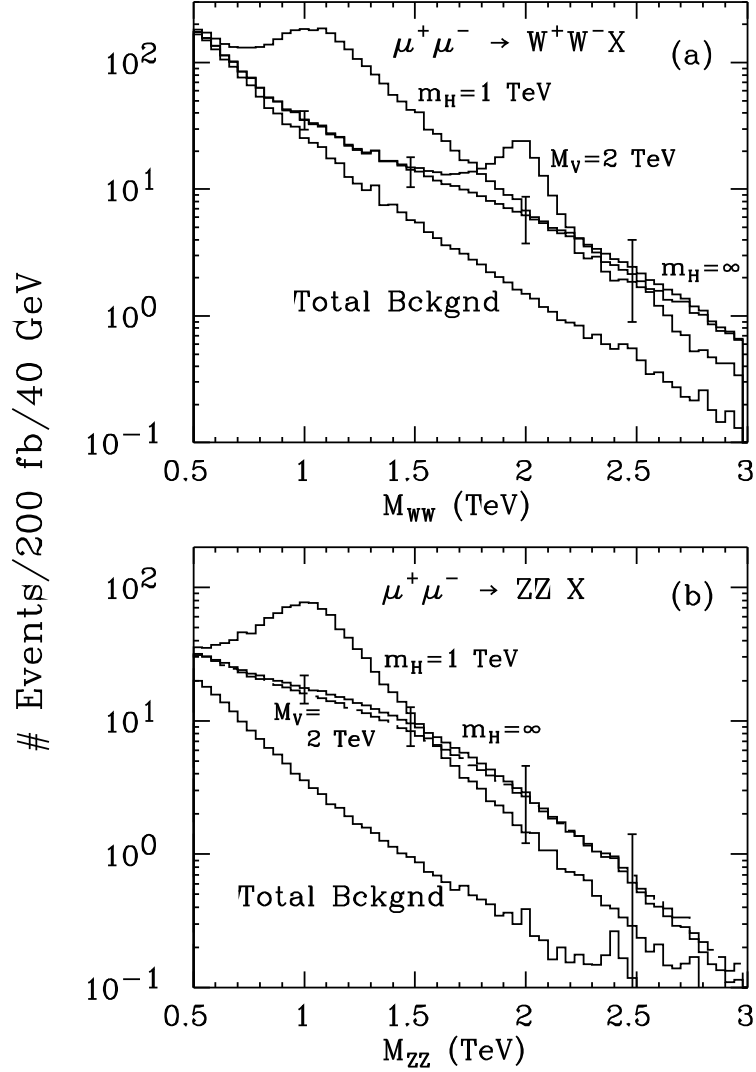


Figure 8: Events as a function of  $M_{VV}$  for sample SEWS models (including the combined backgrounds) and for the combined backgrounds alone in the (a)  $W^+W^-$  and (b)  $ZZ$  final states after imposing all cuts (as listed in the Table 3 caption). Sample signals shown are: (i) the SM Higgs with  $m_{h_{SM}} = 1$  TeV; (ii) the SM with  $m_{h_{SM}} = \infty$  unitarized via K-matrix techniques (LET-K model); and (iii) the Vector model with  $M_V = 2$  TeV and  $\Gamma_V = 0.2$  TeV. (In the  $ZZ$  final state the histogram for (iii) lies slightly lower than that for model (ii) at lower  $M_{VV}$ .) Results are for  $L = 200 \text{ fb}^{-1}$  and  $\sqrt{s} = 4$  TeV. Sample error bars for the illustrated 40 GeV bins are shown in the case of the  $m_{h_{SM}} = \infty$  model.

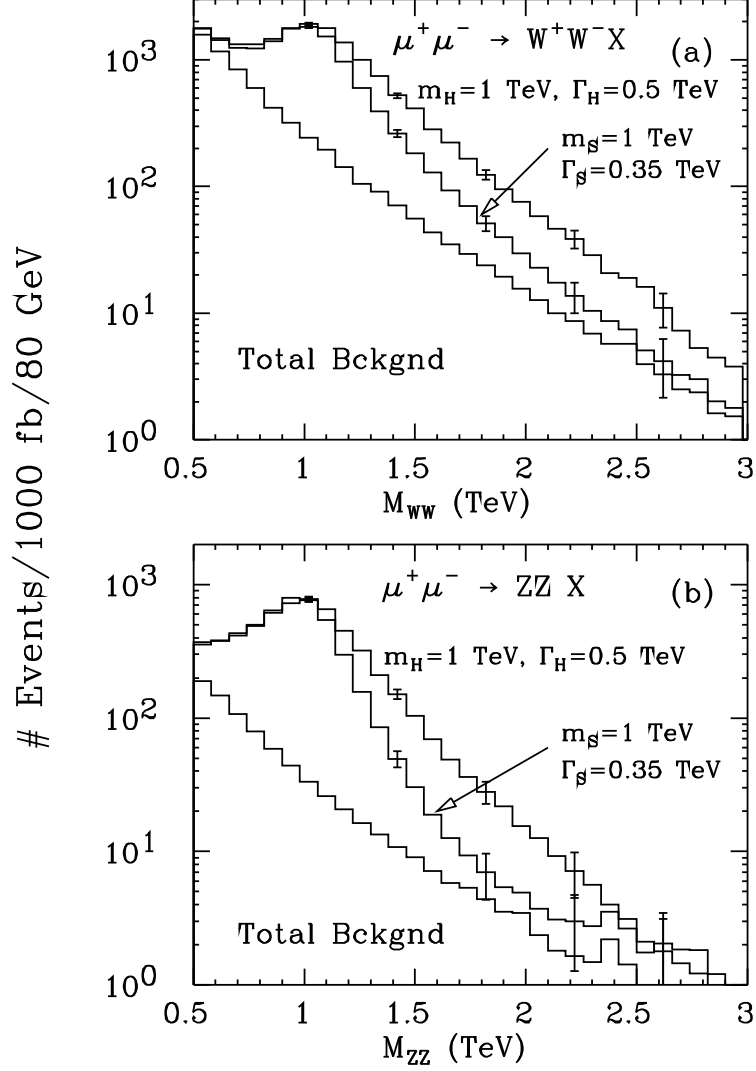


Figure 9: Events as a function of  $M_{VV}$  for two SEWS models (including the combined backgrounds) and for the combined backgrounds alone in the (a)  $W^+W^-$  and (b)  $ZZ$  final states after imposing all cuts. Signals shown are: (i) the SM Higgs with  $m_{h_{SM}} = 1 \text{ TeV}$ ,  $\Gamma_H = 0.5 \text{ TeV}$ ; (ii) the Scalar model with  $M_S = 1 \text{ TeV}$ ,  $\Gamma_S = 0.35 \text{ TeV}$ . Results are for  $L = 1000 \text{ fb}^{-1}$  and  $\sqrt{s} = 4 \text{ TeV}$ . Sample error bars at  $M_{VV} = 1.02, 1.42, 1.82, 2.22$  and  $2.62 \text{ TeV}$  for the illustrated 80 GeV bins are shown.



sonably anticipate accumulating this much luminosity over a period of several years. For  $L = 1000 \text{ fb}^{-1}$ , the accuracy with which the  $M_{VV}$  distributions can be measured becomes very remarkable. To illustrate, we plot in Fig. 9, the signal plus background in the  $m_{h_{SM}} = 1 \text{ TeV}$ ,  $\Gamma_H = 0.5 \text{ TeV}$  SM and the  $M_S = 1 \text{ TeV}$ ,  $\Gamma_S = 0.35 \text{ TeV}$  Scalar resonance model, and the combined background, taking  $L = 1000 \text{ fb}^{-1}$  and using an 80 GeV bin size (so as to increase statistics on a bin by bin basis compared to the 40 GeV bin size used in the previous figures). The error bars are almost invisible for  $M_{VV} \lesssim 1.5 \text{ TeV}$ , and statistics is more than adequate to distinguish between the  $\Gamma_H = 500 \text{ GeV}$  SM resonance and a  $\Gamma_S = 350 \text{ GeV}$  Scalar model at a resonance mass of 1 TeV. Indeed, we estimate that the width could be measured to better than  $\pm 30 \text{ GeV}$ . Further, for such small errors we estimate that a vector resonance could be seen out to nearly  $M_V \sim 3 \text{ TeV}$ . This ability to measure the  $M_{VV}$  distributions with high precision would allow detailed insight into the dynamics of the strongly interacting electroweak sector. Thus, if some signals for a strongly interacting sector emerge at the LHC, a  $\sqrt{s} = 3 - 4 \text{ TeV}$   $\mu^+\mu^-$  (or  $e^+e^-$ , if possible) collider will be essential.

It is important to measure the  $M_{VV}$  spectrum in all three ( $W^+W^-$ ,  $ZZ$  and  $W^+W^+$ ) channels in order to fully reveal the isospin composition of the model. For instance, the Vector model and the LET-K model yield very similar signals in the  $ZZ$  and  $W^+W^+$  channels, and would be difficult to separate without the  $W^+W^-$  channel resonance peak. More generally, the ratio of resonance peaks in the  $ZZ$  and  $W^+W^-$  channels would be needed to ascertain the exact mixture of Vector (weak isospin 1) and Scalar (isospin 0) resonances should they be degenerate. Determination of the isospin composition of a non-resonant model, such as the LET-K model, requires data from all three channels. We emphasize the fact that the  $ZZ$  channel can only be separated from the  $WW$  channels if the jet energy resolution is reasonably good.

### 6.3 Exotic Heavy States

The very high energy of a 4 TeV collider would open up the possibility of directly producing many new particles outside of the Standard Model. Some exotic heavy particles that could be discovered and studied at a muon collider are (1) sequential fermions,  $Q\bar{Q}$ ,  $L\bar{L}$  [40], (2) lepto-quarks, (3) vector-like fermions [41], and (4) new gauge bosons like a  $Z'$  or  $W_R$  [42].

A new vector resonance such as a  $Z'$  or a technirho,  $\rho_{TC}$ , is a particularly interesting possibility. The collider could be designed to sit on the resonance  $\sqrt{s} \sim M_V$  in which case it would function as a  $Z'$  or  $\rho_{TC}$  factory as illustrated in Fig. 10. Alternatively, if the mass of the resonance is not known a priori, then the collider operating at an energy above the resonance mass could discover it via the bremsstrahlung tail. Figure 11 shows the differential cross section in the reconstructed final state mass  $M_V$  for a muon collider operating at 4 TeV for two cases where the vector resonance has mass 1.5 TeV and 2 TeV. Dramatic and unmistakable signals would appear even for integrated luminosity as low as  $L \gtrsim 50 - 100 \text{ fb}^{-1}$ .

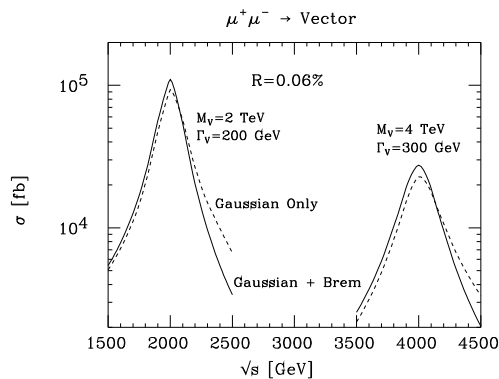


Figure 10: High event rates are possible if the muon collider energy is set equal to the vector resonance ( $Z'$  or  $\rho_{TC}$ ) mass. Two examples are shown here with  $R = 0.06\%$ .

## 7 Conclusions

A muon collider is very likely to add substantially to our knowledge of physics in the coming decades. A machine with energy in the range  $\sqrt{s} = 100\text{--}500$  GeV is complementary to the NLC in that it provides valuable additional capabilities that are best utilized by devoting all available luminosity to the specialized studies that are not possible at the NLC. The most notable of these is the possibility of creating a Higgs boson in the  $s$ -channel and measuring its mass and decay widths directly and precisely. Even if a light Higgs does not exist, studies of the  $t\bar{t}$  and  $W^+W^-$  thresholds at such a low-energy machine would yield higher precision in determining  $m_t$  and  $m_W$  than possible at other colliders. A  $\mu^+\mu^-$  collider with energy as high as  $\sqrt{s} \sim 4$  TeV appears to be entirely feasible and is ideally suited for studying a strongly-interacting symmetry breaking sector, since the center-of-mass energy is well above the energy range at which vector boson interactions must become strong. Many other types of exotic physics beyond the Standard Model could be probed at such a high machine energy. For example, if supersymmetry exists, a 4 TeV  $\mu^+\mu^-$  collider would be a factory for sparticle pair production. Observation of a heavy  $Z'$  in the bremsstrahlung luminosity tail would be straightforward and the machine energy could later be reset to provide a  $Z'$  factory.

## Acknowledgments

This work was supported in part by the U.S. Department of Energy and by the Davis Institute for High Energy Physics.

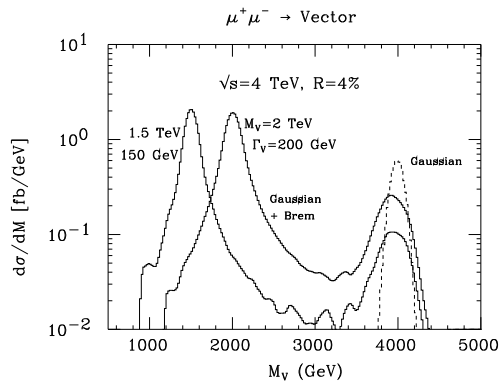


Figure 11: A heavy vector resonance can be visible in the bremsstrahlung tail of a high energy collider. Here a  $\mu^+\mu^-$  collider operating at 4 TeV is shown for  $M_V = 1.5$  TeV and 2 TeV.

## References

1. *Proceedings of the First Workshop on the Physics Potential and Development of  $\mu^+\mu^-$  Colliders*, Napa, California (1992), Nucl. Instru. and Meth. **A350**, 24 (1994).
2. *Proceedings of the Second Workshop on the Physics Potential and Development of  $\mu^+\mu^-$  Colliders*, Sausalito, California (1994), ed. by D. Cline, American Institute of Physics Conference Proceedings 352.
3. *Proceedings of the 9th Advanced ICFA Beam Dynamics Workshop: Beam Dynamics and Technology Issues for  $\mu^+\mu^-$  Colliders*, Montauk, Long Island, (1995), to be published.
4. *Proceedings of the Symposium on Physics Potential and Development of  $\mu^+\mu^-$  Colliders*, San Francisco, California, December 13–15, 1995.
5. A. Tollestrup, these proceedings.
6. R.B. Palmer and A. Tollestrup, unpublished report.
7. D.V. Neuffer, Ref. [2], p. 22.
8. D.V. Neuffer and R.B. Palmer, Ref. [2], p. 70.
9. V. Barger, M.S. Berger, K. Fujii, J.F. Gunion, T. Han, C. Heusch, W. Hong, S.K. Oh, Z. Parsa, S. Rajpoot, R. Thun and B. Willis, *Physics Goals of a  $\mu^+\mu^-$  Collider*, appearing in Ref. [2], p. 55, hep-ph/9503258.
10. G.P. Jackson and D. Neuffer, private communications.
11. V. Barger, M. Berger, J.F. Gunion, and T. Han, preprint UCD-96-12, *Proceedings of the Symposium on Physics Potential and Development of  $\mu^+\mu^-$  Collid-*

- ers, San Francisco, California, December 13–15, 1995.
12. P. Janot, *Proceedings of the 2nd International Workshop on “Physics and Experiments with Linear  $e^+e^-$  Colliders”*, eds. F. Harris, S. Olsen, S. Pakvasa and X. Tata, Waikoloa, HI (1993), World Scientific Publishing, p. 192, and references therein; T. Barklow and D. Burke, private communication.
  13. See “JLC-I”, KEK-92-16, December 1992.
  14. K. Kawagoe, *Proceedings of the 2nd International Workshop on “Physics and Experiments with Linear  $e^+e^-$  Colliders”*, eds. F. Harris, S. Olsen, S. Pakvasa and X. Tata, Waikoloa, HI (1993), World Scientific Publishing, p. 660.
  15. J.F. Gunion, A. Stange, and S. Willenbrock, preprint UCD-95-28 (1995), hep-ph/9602238, to be published in *Electroweak Physics and Beyond the Standard Model*, World Scientific Publishing Co., eds. T. Barklow, S. Dawson, H. Haber, and J. Siegrist.
  16. V. Barger, M. Berger, J.F. Gunion, and T. Han, Phys. Rev. Lett. **75**, 1462 (1995).
  17. V. Barger, M. Berger, J.F. Gunion, and T. Han, UCD-96-6, hep-ph/9602415.
  18. R.B. Palmer, private communication.
  19. H. Haber, R. Hempfling and A. Hoang, CERN-TH/95-216.
  20. M. Carena, J.R. Espinosa, M. Quiros and C.E.M. Wagner, Phys. Lett. **B355**, 209 (1995); J.A. Casas, J.R. Espinosa, M. Quiros and A. Riotto, Nucl. Phys. **B436**, 3 (1995).
  21. J.F. Gunion and H.E. Haber, Phys. Rev. **D48**, 5109 (1993).
  22. Z. Parsa (unpublished).
  23. S. Dawson, appearing in Ref. [3], hep-ph/9512260.
  24. For discussions of the  $t\bar{t}$  threshold behavior at  $e^+e^-$  colliders, see V.S. Fadin and V.A. Khoze, JETP Lett. **46** 525 (1987); Sov. J. Nucl. Phys. **48** 309 (1988); M. Peskin and M. Strassler, Phys. Rev. **D43**, 1500 (1991); G. Bagliesi, *et al.*, CERN Orange Book Report CERN-PPE/92-05; Y. Sumino, *et al.*, Phys. Rev. **D47**, 56 (1992); M. Jezabek, J.H. Kühn, T. Teubner, Z. Phys. **C56**, 653 (1992).
  25. M.S. Berger, talk presented at the *Workshop on Particle Theory and Phenomenology: Physics of the Top Quark*, Iowa State University, May 25–26, 1995, hep-ph/9508209.
  26. P. Igo-Kemenes, M. Martinez, R. Miquel and S. Orteu, CERN-PPE/93-200, Contribution to the *Workshop on Physics with Linear  $e^+e^-$  Colliders at 500 GeV*, K. Fujii, T. Matsui, and Y. Sumino, Phys. Rev. **D50**, 4341 (1994).
  27. C.P. Yuan, talk presented at *Int. Workshop on Elementary Particle Physics: Present and Future*, Valencia, Spain, June 5–9, 1995, hep-ph/9509209.
  28. F. Merritt, H. Montgomery, A. Sirlin and M. Swartz, *Precision Tests of Electroweak Physics*, report of the DPF Committee on Long Term Planning, 1994.
  29. B. Grzadkowski and J.F. Gunion, Phys. Lett. **B350**, 218 (1995).

30. D. Atwood and A. Soni, Phys. Rev. **D52**, 6271 (1995).
31. A. Pilaftsis, Rutherford preprint RAL-TR/96-021.
32. D. Atwood, L Reina and A. Soni, Phys. Rev. Lett. **75**, 3800 (1995).
33. J.F. Gunion, preprint UCD-95-36, hep-ph/9510350, to be published in the Proceedings of the Santa Cruz  $e^-e^-$  Workshop, Santa Cruz, CA, Sept. 4-5, 1995.
34. J.F. Gunion and J. Kelly, Phys. Rev. **D51**, 2101 (1995); and in preparation.
35. M.S. Chanowitz and M.K. Gaillard, Nucl. Phys. **B261**, 379 (1985).
36. J. Bagger, V. Barger, K. Cheung, J.F. Gunion, T. Han, G.A. Ladinsky, R. Rosenfeld, and C.-P. Yuan, Phys. Rev. **D52**, 2878 (1995).
37. V. Barger, K. Cheung, T. Han, and R.J.N. Phillips, Phys. Rev. **D52**, 3815 (1995).
38. D. Burke, these proceedings.
39. V. Barger, M. Berger, J.F. Gunion and T. Han, in preparation.
40. The constraints on a fourth generation in the context of supergravity models can be found in J.F. Gunion, D.W. McKay, and H. Pois, Phys. Rev. **D53**, 1616 (1996).
41. For a recent survey, see V. Barger, M.S. Berger, and R.J.N. Phillips, Phys. Rev. **D52**, 1663 (1995).
42. J.L. Hewett and T.G. Rizzo, Phys. Rep. **183**, 193 (1989).